JOURNAL OF MATERIALS SCIENCE 14 (1979) 712–722

Martensitic transformations in Ti–Mo alloys

R. DAVIS
British Aluminium Co Laboratories, Gerrards Cross, London, UK
H. M. FLOWER, D. R. F. WEST
Department of Metallurgy and Materials Science, Imperial College of Science and Technology, London, UK

A detailed investigation has been made of the structure of alloys of the Ti–Mo system containing up to 10 wt % Mo, water-quenched from the β-phase region. With increase in molybdenum content, the martensite structure changes from hexagonal (α') to orthorhombic (α'') at ~4 wt % Mo, and at 10 wt % Mo, the structure is completely retained β. For alloy compositions <4 wt % Mo, there is a diffusional component in the transformation of the β-phase at the quench rates employed. There is a transition, with increase in molybdenum content, in morphology (from massive to acicular) and in substructure (from dislocations to twins). However, the transitions in crystallography, morphology and sub-structure are not directly related to one another except for an abrupt loss of dislocation substructure at the α'/α'' transition. The α to α'' crystallographic transition has the characteristics of a second order transformation, and evidence has been obtained of the existence of a spinodal within the metastable orthorhombic system. The orthorhombic martensites of Ti–6 and 8 wt % Mo decompose during quenching producing a fine modulated structure within the martensite plates, consistent with a proposed spinodal mode of decomposition.

1. Introduction

The β isomorphous class of titanium alloys, of which titanium–molybdenum is a member, exhibit very simple equilibrium phase diagrams (Fig. 1). However, the transformations of the high temperature b c c β-phase, on cooling, can be complex. Decomposition may proceed via diffusional, shear or mixed diffusional and shear modes. These transformations and their products have been examined previously in very dilute Ti–Mo alloys (containing up to 1% (wt) Mo) [1]. In these alloys the critical cooling rate for 100% transformation to the h c p martensite (α') is not achieved on water-quenching and competitive shear and diffusional transformations take place. Segregation of molybdenum leads to the retention of some β-phase at room temperature. Increasing the molybdenum content decreases both the M_s (Fig. 1) and the critical cooling rate [2, 3] and, therefore, completely shear transformations can take place; β-phase is retained only when the M_f

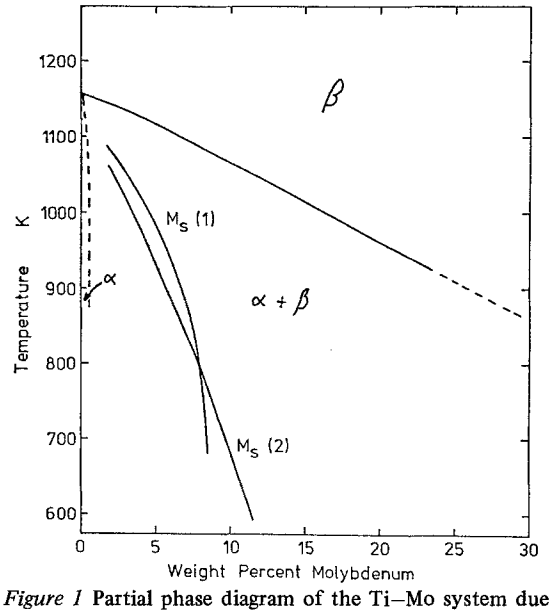

Figure 1 Partial phase diagram of the Ti–Mo system due to Hansen *et al.* [4]. Temperatures corresponding to the start of the martensite transformation M_s (1) due to Duwez; and M_s (2) due to Huang *et al.* [2].

falls below room temperature. Bagariatskii *et al.* [5], using X-ray diffraction, found that in the titanium–molybdenum and other β isomorphous systems, the martensite changes in structure from h c p to orthorhombic (α'') above a critical alloying level (4% for Ti–Mo); this transition in the titanium–molybdenum system was accompanied by a small decrease in hardness. The orthorhombic martensite in a Ti–8% Mo alloy has been shown to be twinned [6–8] whereas the hexagonal form at lower molybdenum levels (e.g. 1% Mo) is generally dislocated [1]. Limited studies of tempering have shown heterogeneous β-phase precipitation in the h c p martensite [1] and homogeneous precipitation in the orthorhombic form [6, 8]. More recent work by the present authors [8] has shown that a metastable spinodal decomposition reaction can occur in the orthorhombic phase.

The range of composition incorporating the h c p/orthorhombic transition is, therefore, of interest and has not hitherto been studied microstructurally. The purpose of the present work was to carry out a systematic study of the microstructure of the martensite as a function of molybdenum content and crystal structure in order to provide a basis for understanding the metastable phase relationships involved and subsequent tempering reactions. The latter will be discussed in detail in a subsequent paper.

2. Experimental procedure

The alloys were made up as 30 g ingots by arc-melting using high purity titanium sponge and molybdenum granules as the basis materials. In view of the negligible change in weight on melting, the molybdenum contents were taken as calculated from the weights of the components used in melting (Table I). The ingots were rolled at 873 K (1173 K for the Ti–8% Mo alloy) to strips of two thicknesses: 0.6 mm for microscopy and 1.2 mm for hardness tests. The strips were cut up to provide suitably sized specimens and the surface oxide was ground off. The specimens were wrapped in molybdenum foil, sealed in silica capsules containing argon and solution treated at 1373 K for 1.8×10^3 sec. After solution-treatment, the specimens were water-quenched. The silica capsules were broken on contact with the water to ensure a rapid quench. The oxygen contents of selected alloys were determined after heat-treatment and taken as an indication of the interstitial contents. Specimens for light and transmission electron microscopy were prepared by electropolishing in a standard solution due to Blackburn and Williams [9]. The light microscopy specimens were etched in a solution of 4% hydrofluoric acid and 16% nitric acid in water. X-ray diffraction was carried out using the Debye Scherrer technique and Cu$K\alpha$ radiation. Specimens for this technique were prepared by electropolishing rods of material to obtain suitably thin cylindrical needle shapes.

TABLE I Alloy Compositions

Alloy	Nominal composition (wt %)	Weighed % Mo	Oxygen content (ppm)
a	Ti–2 Mo	2.0	2300
b	Ti–3 Mo	3.0	2000*
c	Ti–4 Mo	4.0	2800
d	Ti–4 Mo	4.0	2200
e	Ti–4 Mo	4.0	2000*
f	Ti–6 Mo	6.0	3050
g	Ti–6 Mo	6.0	2300
h	Ti–8 Mo	8.0	1850
i	Ti–8 Mo	8.0	2000
j	Ti–10 Mo	10.0	2000*

*Estimated values based on measured oxygen contents of other alloys prepared at the same time.

3. Results

3.1. Light microscopy and X-ray diffraction

All alloys in the range 2 to 8% Mo transformed to martensite on water-quenching from the β-phase field. The Ti–2% Mo alloy exhibited a coarse plate-type martensite (Fig. 2) consisting of large parallel-sided primary plates with partitioned regions filled with progressively smaller secondary plates. In some areas the structure appeared to be more characteristic of "massive" type martensite consisting of lamellar colonies containing several parallel plates. This was observed for both primary and secondary plate structures. With increasing molybdenum content the martensite plate size became finer and more acicular (e.g. Fig. 2). The as-quenched Ti–10% Mo alloy consisted mainly of untransformed equi-axed grains of β-phase.

The crystal structures and lattice parameters of the solution-treated, water-quenched alloys were determined by analysis of the X-ray diffraction patterns. In all cases the high-angle region of the diffraction pattern was partially obscured by fluorescent radiation from the titanium. The

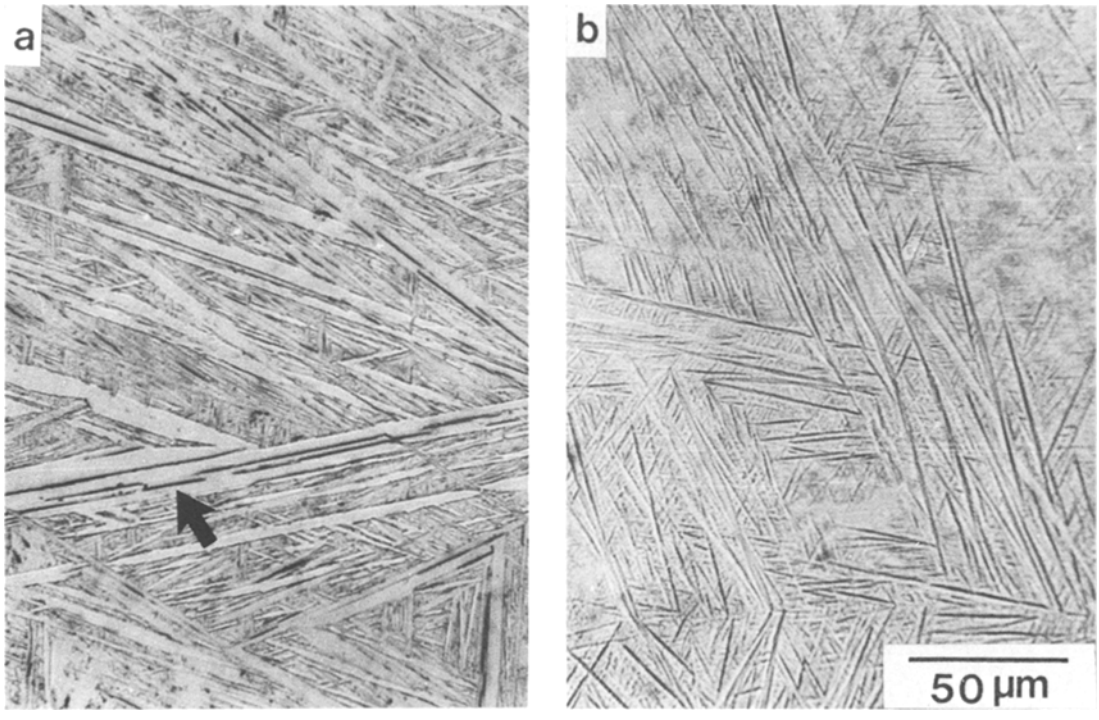

Figure 2 Light micrographs of the martensite in (a) Ti–2% Mo. The arrow shows a lamellar colony consisting of several primary plates. (b) Ti–6% Mo.

martensitic structure of the Ti–2% Mo alloy gave rise to an hexagonal close packed (h c p) diffraction pattern. The strain in the lattice resulting from the martensitic transformation caused slight broadening of the high-angle lines, but the lines could still be distinguished against the dark background originating from fluorescent radiation. No lines due to the β-phase were observed. The diffraction pattern from the Ti–4% Mo alloy was similar, except that low- and high-angle lines had broadened with the result that the high-angle lines were difficult to distinguish against the background fluorescent radiation. The diffraction patterns from the Ti–6% and 8% Mo alloys were notably different and were characterized by splitting of all lines, seen in the previous hexagonal diffraction patterns, other than the $\{0\,0\,n\}$ lines. These results were consistent with a change in crystal symmetry from hexagonal to orthorhombic at compositions greater than 4% Mo. The splitting of the diffraction lines was greater for the Ti–8% Mo alloy as a result of an increased orthorhombic distortion. In both the Ti–6 and 8% Mo alloys, the high-angle lines were obscured due to broadening and fluorescent radiation, and no lines due to the β-phase could be detected.

The planar spacings were determined from the diffraction lines which could be accurately measured. The accuracy of the lattice parameters, which were determined from the available planar spacings, was limited as it was impossible to measure accurately the high-angle diffraction lines. The lattice parameter values for each alloy are given in Table II. The difference in interstitial content, as indicated by the oxygen contents, between different melts of the same alloy made no measurable difference to the as-quenched crystal structures or the lattice parameters. The only detectable microstructural change was a decrease

TABLE II Lattice parameters (Å) of the solution treated and water-quenched alloys. (Accuracy of values ± 0.010.)

Alloy composition (wt %)		*a*	*b*	*c*	*c/a*	*b/a* $\sqrt{3}$
Ti–2 Mo	hex. α'	2.945		4.681	1.590	1
Ti–4 Mo		2.943		4.676	1.589	1
Ti–6 Mo	ortho. α''	2.965	5.045	4.662		0.982
Ti–8 Mo		2.994	4.990	4.644		0.962

in martensite plate size with increased interstitial content.

3.2. Hardness measurements

The change in hardness with molybdenum content of the as-quenched structure for alloys with a similar interstitial content (e.g. alloys a, d, g and i) followed a similar trend to that reported previously [5, 10, 11]. A maximum in hardness was observed around 4% Mo and a minimum around 8% Mo (Fig. 3). Beyond 8% Mo the hardness increases rapidly. For a given molybdenum content the hardness was found to increase markedly with increased interstitial content (e.g. alloys c and f).

3.3. Electron microscopy

Electron microscopy confirmed the morphological changes with molybdenum content observed by light microscopy. It was additionally found that even in the 4% Mo alloy some colony structures were still present. The sub-boundaries between the individual plates in such a region frequently contained a thin layer of β-phase. Similar, but more predominant β layers have previously been reported in more dilute Ti–Mo alloys [1, 12]. The β layers lay within complex networks of dislocations which consisted predominantly of [0 0 0 1] Burgers vectors with lesser numbers of $\frac{1}{3}\langle 1\,1\,\bar{2}\,3\rangle$ and $\frac{1}{3}\langle 1\,1\,\bar{2}\,0\rangle$ types. The α'- and β-phases were related by the usual Burgers orientation relationship and the sub-boundary plane was close to the $\{4\,3\,3\}_\beta$ normally associated with this relationship. Neighbouring martensite plates were frequently found to be $\{1\,0\,\bar{1}\,1\}$ twin-related. Such a relationship can be obtained when two specific variants of the Burgers relationship are adopted by the martensite nuclei.

The substructure of the martensite plates changed progressively with increasing molybdenum content from dislocation tangles in which Burgers vectors of the type $\frac{1}{3}\langle 1\,1\,\bar{2}\,0\rangle$ and $\frac{1}{3}\langle 1\,1\,\bar{2}\,3\rangle$ were observed, to a structure consisting of $\{1\,0\,\bar{1}\,1\}$ twins together with stacking faults. It should be emphasized that the substructural transition was not abrupt – a few twinned plates were observed in the 2% Mo alloy and a few dislocated plates in the 4% Mo alloy. Furthermore, some individual plates contained both twins and dislocated plates in the 4% Mo alloy. Furthermore, some individual plates contained both twins and dislocations (e.g. Fig. 4).

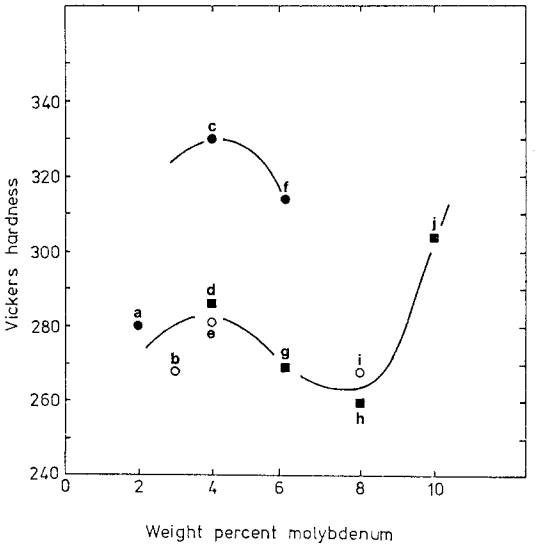

Figure 3 Vickers hardness after solution treatment at 1373 K for 1.8×10^3 sec. The letters correspond to the different alloys shown in Table I.

The orthorhombic martensites of the 6 and 8% Mo alloys were distinctively different from the hexagonal forms. The microstructure was entirely acicular and contained no β-phase (Fig. 5). The individual plates were dislocation-free and contained twins and stacking faults. Fig. 5a shows a typical Ti–6% Mo martensite plate containing twins and stacking faults, both of which are viewed approximately edge on. Fig. 5b clearly indicates that the twin plane is of the $\{1\,1\,1\}_{\alpha''}$ type which is derived from the $\{1\,0\,\bar{1}\,1\}$ twin plane of the hexagonal form. The fault plane in this case is also of the $\{1\,1\,1\}_{\alpha''}$ type since the trace of the edge-on faults lies perpendicular to the parent $(\bar{1}\,1\,1)_{\alpha''}$ reciprocal lattice vector. Although only $\{1\,1\,1\}_{\alpha''}$ twinning was ever observed, ribbon-like stacking faults lying on several crystallographically different planes were occasionally observed. Fig. 6 shows this type of fault in the 8% Mo alloy. Clearly the edge-on fault components lie on the $(0\,0\,1)_{\alpha''}$ plane derived from the basal plane of the hexagonal phase. Single surface trace analysis indicated that some faults also lay on fault planes derived from the $\{1\,0\,\bar{1}\,1\}$, $\{\bar{2}\,1\,1\,2\}$ and $\{1\,\bar{3}\,2\,0\}$ hexagonal planes.

Differences in oxygen content made no difference to the martensite morphology or substructure, as observed by electron microscopy.

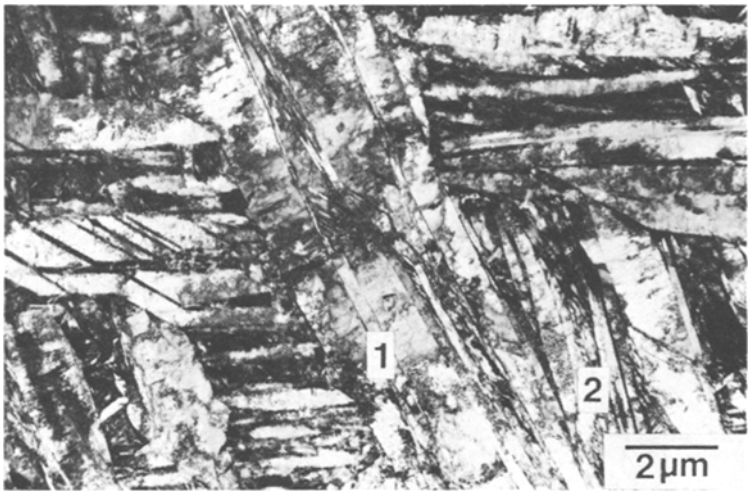

Figure 4 Ti–2% Mo. Electron micrograph showing the general morphology of the martensite. Areas show lamellar colonies typical of the massive type martensite for both primary plates (1) and secondary plates (2). Although the substructure within the plates consists predominantly of dislocations, some twinning is also evident.

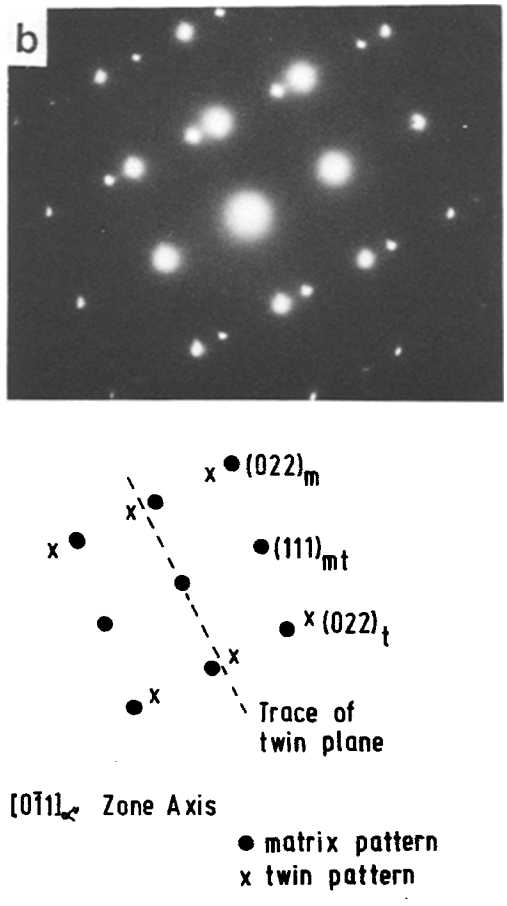

Figure 5 Ti–6% Mo. Part of a martensite plate internally twinned on the (1 1 1) plane. (a) Bright-field micrograph. (b) Selected-area diffraction pattern showing the twin relationship.

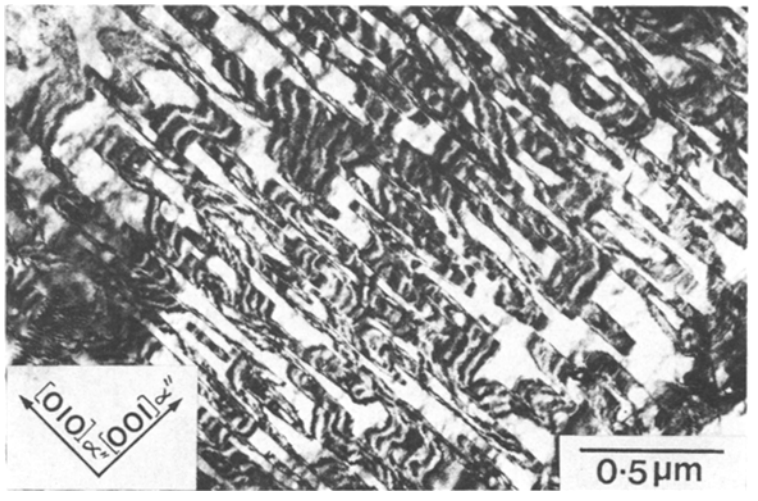

Figure 6 Ti–8% Mo. Ribbon-like stacking faults within a martensite plate. Arrows indicate the direction of the plane normals.

3.4. Decomposition of the martensites during quenching

In the hexagonal Ti–2 and 3% Mo alloys there was no evidence of decomposition within the martensite plates, although the presence of β layers in some of the plate boundaries indicated a partly diffusional nature to the transformation on quenching. The orthorhombic alloys, however, exhibited a fine modulated structure within the martensite plates. Only two variants of the modulated structure were observed in any one plate, implying that it had formed after the martensite transformation. The modulated structure gave rise to diffuse satellite reflections about the main reflections in the diffraction patterns. Fig. 7 shows the modulated structure observed in a martensite plate of the Ti–80% Mo alloy. The modulations were continuous up to the martensite plate or twin interfaces. Similar but much less clearly developed structures were observed in the Ti–4% Mo alloy.

4. Discussion

4.1. Crystallography

The normally accepted lattice correspondence between the b c c and h c p forms of titanium is that due to Burgers [13] and results in the observed Burgers' relationship between α'- and β-phases in $(0\,0\,0\,1)_{\alpha'} \| (0\,1\,1)_{\beta}$ $\langle 1\,1\,\bar{2}\,0\rangle_{\alpha'} \sim \| \langle 1\,1\,\bar{1}\rangle_{\beta}$. The present results are entirely consistent with this. The transformation of β to α', using the Burgers relationship, can be achieved via a 10% contraction along $[1\,0\,0]_{\beta}$ which corresponds to $[2\,\bar{1}\,\bar{1}\,0]_{\alpha'}$, a 10% expansion along $[0\,1\,\bar{1}]_{\beta}$ which corresponds to $[0\,1\,\bar{1}\,0]_{\alpha'}$ and a 1% expansion along $[0\,1\,1]_{\beta}$ which corresponds to $[0\,0\,0\,1]_{\alpha'}$. In the case of

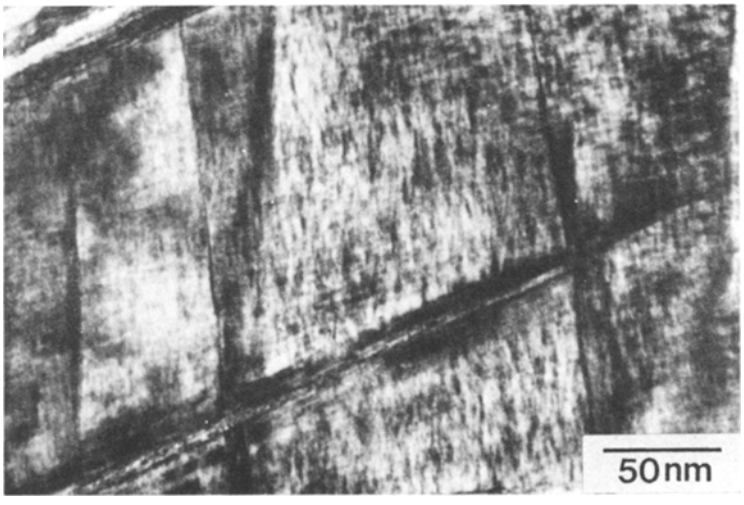

Figure 7 Ti–8% Mo. The modulated structure within a martensite plate, formed during quenching.

TABLE III Values of principal strains, $\epsilon_i = \eta_i - 1$, for Ti and Ti–Mo martensites

Alloy composition (wt%)	Structure	ϵ_1 (%)	ϵ_2 (%)	ϵ_3 (%)
Ti	Hexagonal	−10.1	10.1	0.90
Ti–2 Mo	Hexagonal	−10.2	10.0	0.91
Ti–4 Mo	Hexagonal	−10.2	10.0	0.91
Ti–6 Mo	Orthorhombic	−9.5	8.9	0.65
Ti–8 Mo	Orthorhombic	−8.5	7.8	0.37

$\eta_1 = a/a_\beta$, $\eta_2 = b/\sqrt{2}a_\beta$, $\eta_3 = c/\sqrt{2}a_\beta$

transformation to α'' the equivalent lattice correspondence is: $[1\,0\,0]_\beta$ and $[1\,0\,0]_{\alpha''}$, $[0\,1\,\bar{1}]_\beta$ and $[0\,1\,0]_{\alpha''}$, $[0\,1\,1]_\beta$ and $[0\,0\,1]_{\alpha''}$. The corresponding strains are slightly reduced (as discussed below).

The martensite transformations in titanium and its alloys are therefore unusual (as noted by Kelly and Groves [14]) in that the geometric conditions for the lattice deformation to be an invariant plane strain are almost satisfied. In terms of the principal strains, $\epsilon_i = \eta_i - 1$, one value of ϵ_i must be zero and the other two have opposite signs. Table III gives the computed values of the principal strains (ϵ_i) for pure titanium and for the Ti–Mo alloys studied. The calculations were made from the relations $\eta_1 = a/a_\beta$, $\eta_2 = b/\sqrt{2}a_\beta$, $\eta_3 = c/\sqrt{2}a_\beta$, where a, b, c are the parameters of the orthorhombic cell of the martensite, and a_β is the lattice parameter of the β-phase. It can be seen that (i) ϵ_3 is small for all the martensite structures, and (ii) for the orthorhombic martensites of high molybdenum content all three principal strains are reduced compared to those for the hexagonal martensites.

The lattice parameters of the b c c β cell were obtained from the values cited by McQuillan and McQuillan [15]. The lattice parameter of pure β titanium at 1173 K is given as 3.3132 Å and at 293 K as 3.283 Å. The latter value was obtained by extrapolating to zero alloy content. McQuillan and McQuillan also stated that for Ti–Mo alloys there is a decrease in a of 0.0023 Å per atomic per cent molybdenum. These values are in good agreement with the more recent lattice parameter values for Ti–Mo alloys obtained by Hake *et al.* [16]. Using the high and low temperature value of a_β from [15], an overall coefficient of linear expansion was calculated and found to be 1.0×10^{-5}. The coefficients of linear expansion in α-titanium were also given as 1.1×10^{-5} in the a direction and as 1.3×10^{-5} in the c direction, up to 973 K, although there is some question over the accuracy of the latter value [15]. Assuming that these coefficients approximately apply for the alloyed hexagonal, and orthorhombic cells, the transformation strains involved at the M_s temperature for each alloy are approximately the same as those calculated using the room temperature lattice parameters.

The orthorhombic α'' structure is intermediate between the b c c and h c p structures and hence the $\beta \rightarrow \alpha''$ transformation involves smaller principal strains than those required to produce the h c p structure. The reduction in the observed principal strains is small in the case of the titanium–molybdenum system since the orthorhombic structure is close to the h c p α' cell. It is interesting to note that in the analogous titanium–tantalum system the production of orthorhombic martensite involves a continuous decrease in the principal strains with increasing composition [17] until at a composition of Ti–53.2% Ta, all three principal strains are less than 3%, which resulted in an orthorhombic crystal structure approximating to the b c c β-phase from which it was formed.

An explanation for change in crystal structure from α' to α'' is given by Brown *et al.* [18]. In the orthorhombic martensite of the titanium–niobium system they found no evidence for segregation of niobium to special sites, and showed that the crystal structure gave an eight-fold co-ordination around each (Ti, Nb) atom, with four additional neighbours at a slightly greater distance. Both atoms have a Goldschmidt atomic radius of 1.47 Å and, therefore, difference in size is unlikely to account wholly for the distortion to orthorhombic symmetry. It was suggested that the distortion was a reflection of a tendency for niobium to retain the eight-fold co-ordination obtained in the b c c form.

Similarly, the change in crystal structure in the titanium–molybdenum martensites with increasing molybdenum content can be regarded as a change in the nearest neighbour co-ordination from twelve in the h c p structure to approximately eight in the orthorhombic structure. With increasing molybdenum (1.40 Å [19]) is very close to that of for an eight-fold co-ordination, and the closer is the final orthorhombic cell to the original b c c β cell. Also the Goldschmidt atomic radius of molybdenum (1.40 [19]) is very close to that of titanium and size difference effects should again be small. The form of the equilibrium diagram and

the decrease in M_s with increasing molybdenum content are consistent with the above suggestions for the change in martensite symmetry.

The present results confirm the earlier finding of Bagariatskii *et al.* [5] that the crystallographic transition to orthorhombic symmetry takes place at 4% Mo. The earlier results [5] also showed that beyond 4% Mo there is a steady change in the *a*, *b* and *c* parameters of the orthorhombic cell away from those of the h c p structure towards those of the b c c phase, i.e. there is no discontinuity in molar volume at the transition. This strongly suggests that the α'/α'' transition is second order in type and the free energy curve for α'' must join the α' curve smoothly as shown at c_1 in Fig. 8. The α'' curve is shown as passing through a maximum and then falling towards the β curve as its parameters change towards those of the b c c phase. The two curves cross at a point which defines the upper temperature (T_0) and composition (c_3 in Fig. 8) limits for α'' martensite formation. This temperature is clearly above room temperature for all the alloys studied in this work except for the 10% Mo samples which remained predominantly β-phase after water-quenching. In the analogous titanium–niobium [5] and titanium–tantalum [17] systems there is also good evidence for second order transformation between the α' and α'' phases. In the latter case the close approach of the α'' lattice parameter to those of the β-phase at the composition at which T_0 drops below room temperature indicates the possibility that the α''/β transition may also be second order. Whether or not this is true for titanium–tantalum alloys or the other β isomorphous titanium alloys, the overall form of the free energy diagram suggested here indicates the existence of a spinodal in the metastable orthorhombic free energy curve (at c_2 in Fig. 8).

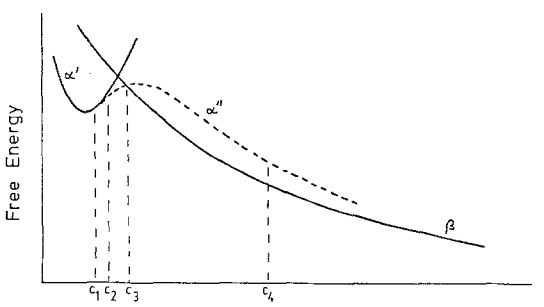

Figure 8 Proposed form of free energy curves for α', α'' and β-phases at a temperature T_0, representing the upper temperature limit for α'' formation.

4.2. Martensite morphology

In the present investigation both massive and acicular martensites have been observed. Molybdenum is very effective in producing the acicular type martensite, and very little massive martensite has previously been reported in the as quenched structure of Ti–0.5% Mo [1]. However, the transition from massive martensite to plate martensite is not complete until a molybdenum content of ~4% Mo is reached. Some of the larger martensite plates of the Ti–4% Mo alloy (M_s = 973 K) were up of a number of parallel plates separated by sub-boundaries which represents a morphology intermediate between massive colonies and the single crystal acicular martensite plate. However, in Ti–6% Mo (M_s = 883 K) no such sub-boundaries were observed, showing that the martensite was entirely acicular. The completion of the transition is consistent with the published results for several titanium alloys [20] where the transition in martensite morphology occurs around an M_s temperature of 923 to 973 K. However, as pointed out in that work the transition in morphology cannot be explained on the basis of the M_s alone, and many other factors have to be considered [21, 22].

The factors involved in the transition from lath → acicular martensite in iron alloys have been discussed by Krauss and Marder [23] who concluded that the morphological transition is due to complex shear interactions, which have received little attention in the literature. Qualitative evidence points to the transition being related to the temperature dependence of plastic deformation mechanisms in the parent austenite as well as to the product martensite structures in a given alloy system. Flower *et al.* [24] suggested that massive martensite forms when slip occurs in the β-phase ahead of the α' plate to reduce the shape strain. When solid-solution strengthening and lowering of the M_s sufficiently strengthen the β-phase to prevent slip, normal plate-like martensite is obtained. Flower *et al.* [1] suggested that diffusion may also contribute to the reduction of the shape strain during water-quenching from the β-phase field of very dilute Ti–Mo alloys, e.g. Ti–0.5 and 1.0% Mo.

In the present study the specimens were solution-treated in bundles sealed in silica tubes, which were broken on contact with water to ensure a fairly rapid quench. After taking all factors into account it is estimated that the quench rate was at

TABLE IV Critical cooling rates (CCR) for dilute Ti–Mo alloys

Mo	0	1	2	3	4	6	8
M_s (K)	1348	>1072	1053	1013	973	883	788
CCR ($K\,sec^{-1}$)	3000	420	360	290	220	130	70

M_s values from [2]. CCR values from [3]. Values for pure Ti from [26].

least 200 $K\,sec^{-1}$. Table IV gives the critical cooling rate for avoiding diffusional transformations for various titanium–molybdenum alloys determined by Huang *et al.* [3]. Assuming that the estimated quench rate applies to all specimens, it can be seen that alloys containing 4% Mo and less have been quenched insufficiently fast to prevent a diffusional component in the transformation. The precise effect of the diffusional component on the martensite transformation is not known, but must play a part in the nucleation and growth of the resulting structure, because at this cooling rate previous work [3] indicates that the diffusional curve of the CCT diagram may well be crossed first. For slightly faster cooling rates, the M_s is crossed first, but the diffusional curve may be crossed before M_f is reached. Therefore, there will be a diffusional component of the transformation following the martensite nucleation. Since it is well established that the α' formed in β by shear or diffusion both exhibit the same orientation relationship and habit plane it is possible (as discussed by Flower *et al.* [1]) that the transition from diffusional to shear growth, or vice versa, is not sharply defined and the relative contribution of shear and diffusion to the growth of the α' plates cannot be distinguished.

The thin layers of β-phase, which have been observed along the sub-boundaries within the large martensite plates of the Ti–2, 3 and 4% Mo alloys are considered to result from the diffusional component of the transformation. These β layers form as a result of molybdenum segregation to the β-phase ahead of the advancing α' plate interface stabilizing the β against transformation during the quench.

The transition from massive to acicular morphology in other titanium alloy systems has been reported to occur when the alloying addition exceeds a certain value [20], e.g. 2.4% Cr, 6% Cu, 20% Zr. The critical cooling rates [3] are respectively 350, 320 and 320 $K\,sec^{-1}$. The quench rates employed may not have exceeded the critical cooling rates for alloy additions less than the transition values, which would result in a diffusional contribution to the transformation.

The present results, taken in conjunction with those of other workers, discussed above, suggest that diffusion plays a significant role in the formation of massive martensitic structures in titanium–molybdenum and other titanium alloys. The presence of colonies of secondary plates with massive morphology (Fig. 3) between primary acicular martensite plates may be explained by a local decrease in cooling rate due to the release of latent heat as the primary plates are formed.

4.3. Martensite substructure

Within the hexagonal martensites there is a steady increase in the number of twinned martensite plates as the molybdenum content is raised from 2%, at which level the substructure consists predominantly of dislocations. This indicates a change in lattice invariant shear mode from slip to twinning as molybdenum content increases and M_s decreases. The substructural change, however, is gradual and is incomplete at the point of crystallographic transition from α' to α''. The incidence of twinning cannot, therefore, be directly related to changes in martensite morphology or to the crystallographic transition. As in many other alloy systems the change from a slipped to a twinned sub-structure appears to be related to the M_s temperature. As the M_s decreases, the diffusional contribution to relief of stress in the β-phase ahead of an advancing martensite plate decreases and shear modes must increasingly account for the changes in shape accompanying the transformation. In this context it may be noted that the frequent observation of $\{1\,0\,\bar{1}\,1\}$ twin related pairs of plates is consistent with this since the shape strain of such a pair is lower than that for other alternative Burgers related variants. However, as the nuclei grow apart on their separate habit planes, the strains must be accommodated individually. Initially, slip provides the lattice invariant shear but as molybdenum content is raised and the M_s decreases, the critical resolved shear stress for twinning falls while that for slip increases. Thus an increasing fraction of the lattice invariant shear is accommodated by twinning.

The h c p to orthorhombic transition produces an abrupt termination to slip which is replaced entirely by $\{1\,1\,1\}_{\alpha'}$ twinning and faulting. This may indicate increased ease of twinning relative to

slip in the lower symmetry crystal system. The $(1\,1\,1)_{\alpha''}$ twins are equivalent to the $\{1\,0\,\bar{1}\,1\}_{\alpha'}$ twins observed in the hexagonal martensites and clearly serve the same role. The presence of the faulting is more difficult to account for since it appears on several crystallographically different planes and cannot be positively identified as a lattice invariant shear mode.

4.4. Decomposition of the martensites during quenching

The retention of small amounts of β-phase at plate boundaries in the hexagonal martensites has already been discussed above and is not considered further here. The observation of modulated structures within the orthorhombic martensite plates clearly indicates that the martensite itself has begun to decompose during the quench. From the M_s values shown in Fig. 1 this decomposition must have begun below about 900 K, and hence must be extremely rapid. This, together with the regularity of the structure and the continuity of the modulations up to high-angle interfaces is suggestive of spinodal decomposition. Previously reported work by the present authors [8] has shown that such decomposition does occur on ageing the orthorhombic martensites of the titanium–molybdenum and two other (titanium–vanadium, titanium–niobium) systems. These observations are in agreement with the proposed form of α'' free energy curve shown in Fig. 8.

4.5. Hardness and the role of oxygen

The change in hardness with increasing molybdenum content follows a similar trend to that shown in previous work [5, 6, 10, 11].

The addition of 4% Mo to pure titanium leads to an increase in hardness of ~100 HV. The small difference in atomic radii is unlikely to account for such a large solution hardening effect. Molybdenum is a strong β stabilizer and exhibits only a very limited solubility in the equilibrium hexagonal α-phase. The high solid-solution hardening is most likely related to the electronic interaction of the solute and solvent atoms.

Over the composition range 4 to 8% Mo, a small decline in hardness is observed. It is difficult to account for this decline as a number of factors will affect the hardness in this range. Firstly, the crystal structure is orthorhombic and less strain is involved in the transformation (Table III) which will lead to less work hardening of the final martensite structure due to a smaller lattice invariant strain. Secondly, a transition from a dislocated to twinned substructure occurs which may also lead to a drop in hardness. On the other hand, the effect of solid-solution strengthening has to be taken into account. Finally, the martensites in this composition range decompose during the quench such that they contain a fine modulated structure which may lead to an increase in hardness above that of an undecomposed structure.

The hardness rises rapidly at ~10% Mo due to the dispersion-hardening of the β-phase by the formation of the ω-phase during the quench [10, 11].

Fig. 2 illustrates clearly that increasing the oxygen level from roughly 2000 to 3000 ppm produces hardness increases greatly in excess of the variations due to molybdenum content. This is consistent with the well established role of oxygen as a potent interstitial solid-solution hardening element in titanium. In this regard its behaviour is similar to that of carbon in iron. It has been suggested [25] that oxygen may promote the orthorhombic distortion of titanium alloy martensites via an ordered occupancy of interstitial sites in much the same way that carbon causes a tetragonal distortion in iron-based systems. However, there is no indication in the present work that the crystallographic transition is influenced by a 50% change in oxygen content: the transition consistently occurs at a molybdenum content of 4%.

5. Conclusions

(1) The alloys Ti–2 to 8% Mo transform to martensite on quenching from the β-phase field. In the Ti–10% Mo alloy, the β-phase is largely retained.

(2) For compositions <4% Mo the crystal structure of the martensite is h c p, and for compositions >4% Mo, orthorhombic. The three principal strains to form the orthorhombic martensite are less than those required to form the hexagonal martensite, and the lattice parameters lie between those for the b c c β and the h c p α' cell.

(3) Molybdenum is very effective in producing acicular martensite. The transition from massive to acicular martensite is complete above 4% Mo. With increasing molybdenum content a transition in the martensite substructure occurs, from dislocated to twinned and faulted. The transition in martensite morphology, substructure, and crystallography are not directly related to one another with the exception of the abrupt loss of dislocation

substructure at the α'/α'' transition.

(4) The transformation on quenching for alloy compositions <4%Mo contains a diffusional component at the quench rates employed, which may be an important factor for the formation of massive martensite.

(5) The α' to α'' crystallographic transition has the characteristics of a second order transformation. The proposed form of the free energy/composition relationship indicates the existence of a spinodal within the metastable orthorhombic phase diagram.

(6) The orthorhombic martensites of Ti–6 and 8%Mo decompose during quenching producing a fine modulated structure within the martensite plates. The microstructure is consistent with a spinodal mode of decomposition of the orthorhombic phase.

Acknowledgements

The authors would like to thank Professor J. G. Ball for the provision of research facilities and Imperial Metal Industries for the supply of titanium. The award of an S.R.C. research studentship to one of the authors (R. D.) is gratefully acknowledged.

References

1. H. M. FLOWER, S. D. HENRY and D. R. F. WEST, *J. Mater. Sci.* 9 (1974) 57.
2. Y. C. HUANG, S. SUZUKI, H. KANEKO and T. SATO, "The Science, Technology and Application of Titanium", edited by R. I. Jaffee and N. Promisel (Pergamon Press, London, 1970) p. 691.
3. *Idem, ibid,* p. 695.
4. M. HANSEN, E. L. KAMEN, H. D. KESSLER and D. J. McPHERSON, *Trans. AIME* **191** (1951) 882.
5. I. A. BAGARIATSKII, G. I. NOSOVA and T. V. TAGUNOVA, *Sov. Phys. Doklady* **3** (1959) 1014.
6. J. C. WILLIAMS and B. S. HICKMAN, *Met. Trans.* **1** (1970) 2648.
7. D. W. JAMES and D. M. MOON, "The Science, Technology and Application of Titanium", edited by R. I. Jaffee and N. Promisel (Pergamon Press, London, 1970) p. 767.
8. H. M. FLOWER, R. DAVIS and D. R. F. WEST, Proceedings of the Third International Conference Titanium, Moscow 1976 (to be published).
9. M. J. BLACKBURN and J. C. WILLIAMS, *Trans. Met. Soc. AIME* **239** (1967) 287.
10. A. B. KOLACHEV and V. S. LIASOTSKAYA, "Titanium Science and Technology", edited by R. I. Jaffee and H. M. Burke (Plenum Press, New York, 1973) p. 1569.
11. L. N. GUSEVA and I. V. EGIZ, *Met. Sci. Heat. Treat.* **16** (1974) 355.
12. R. G. NICHOLS, H. M. FLOWER and D. R. F. WEST, *J. Mater. Sci.* 8 (1973) 261.
13. W. G. BURGERS, *Physics* **1** (1934) 561.
14. A. KELLY and G. W. GROVES, "Crystallography and Crystal Defects", (Longman, London, 1970).
15. A. D. McQUILLAN and M. McQUILLAN, "Titanium" (Butterworths, London, 1956).
16. R. R. HAKE, D. H. LESLIE and T. G. BERLINCOURT, *J. Phys. Chem. Solids* **20** (1961) 177.
17. K. A. BYWATER and J. W. CHRISTIAN, *Phil. Mag.* **25** (1972) 1249.
18. A. R. G. BROWN, D. CLARK, J. EASTABROOK and K. S. JEPSON, *Nature* **201** (1964) 914.
19. C. J. SMITHELLS, "Metals Reference Book" (Butterworths, London, 1967).
20. S. BANERJEE and R. KRISHNAN, *Met. Trans.* 4 (1973) 1811.
21. S. BANERJEE, S. J. VIJAYAKER and R. KRISHNAN, "Titanium Science and Technology", edited by R. I. Jaffee and H. M. Burke (Plenum Press, New York, London, 1973) p. 1597.
22. S. BANERJEE and R. KRISHNAN, *Acta Met.* **19** (1971) 1317.
23. G. KRAUSS and A. R. MARDER, *Met. Trans.* 2 (1971) 2343.
24. H. M. FLOWER, P. R. SWANN and D. R. F. WEST, *J. Mater. Sci.* 7 (1972) 929.
25. C. HAMMOND, *Scripta Met.* 6 (1972) 569.
26. M. CORMIER and F. CLAISSE, *J. Less Common Metals* 34 (1974) 181.

Received 20 June and accepted 21 July 1978.